Fluoro-Modified Surface

Subjects: Materials Science, Coatings & Films

Contributor: Yuanzhe Li , Zhe Cui , Qiucheng Zhu , Srikanth Narasimalu , Zhili Dong

The original fluoro-modified polyurethane encapsulated process was designed to rapidly fabricate low flow-resistance surfaces on the zinc substrate. For the further enhancement of the drag-reduction effect, chemical etching was introduced during the fabrication process, and its surface morphology, wettability, and flow-resistance properties in a microchannel were also studied in this paper. It is indicated that the zinc substrate with micro-nano scale roughness obtained by Cu^{2+} assisted nitric acid etching was super hydrophilic. However, after the etched zinc substrate encapsulated with fluoro-polyurethane, the superhydrophobic wettability can be obtained. As this newly fabricated surface being applied into the microchannel, it was found that with the increase of Reynolds number, the drag reduction rate of the superhydrophobic surface remained basically unchanged at 4.0 % compared with the original zinc substrate. Furthermore, the prepared superhydrophobic surfaces exhibited outstanding reliability in most liquids, and such chemical-etching methodology were capable to be commercialized in the piping as well as the coating industry.

chemical etching enhancement surface nano-structures fluoropolyurethane zinc substrate drag reduction

1. Introduction of Industrial Pipeline Drag-Reduction Technology

Industrial pipeline drag reduction technology has been in existence for a long time, and the modern superhydrophobic interface undoubtedly provides a new research direction for drag reduction. Therefore, the efficient preparation of superhydrophobic surfaces may generally include (1) constructing suitable micro/nanostructures on low surface energy materials or (2) modifying surfaces with low surface energy materials [1].

Except for the modification of surface materials, the surface microstructure could also provide an important methodology for surface modification. The microstructure of lotus leaves and shark-skin surfaces have been analyzed in recent years. Studies also have shown that these microstructure surfaces indicate good superhydrophobic and self-cleaning effects [2]. In 1997, German botanists Barthlott and Neinhuis [3] referred to this characteristic of the lotus leaf as the Lotus Effect. Cottin et al. [4] found that the superhydrophobic surface of this micro/nanostructure can significantly reduce the flow resistance as well. Many researchers have developed superhydrophobic surfaces by analyzing the surfaces of plant leaves, whose slipping phenomenon could significantly reduce the flow resistance. What is more, various experimental approaches are capable of creating

such a microstructure interface, which includes template methods, plasma texturing, lithography [5][6], and chemical deposition at present. However, the preparation process of the template method, which requires pre-preparation of the template, is so complicated that has not been widely used yet [7][8]. The processing of plasma texturing with the thermal oxidation method takes so much time, and it is applicable for limited substrate materials. Although the plasma-induced nanotexture is uniform and indicates outstanding superhydrophobic wettability in the recent work of K. Ellinas et al., the good attachment of plasma fluorocarbon deposition could be obtained in polymer substrate only [9]. It is still easy to be scratched, which needed to be further enhanced with more than one polymeric layer on the commonly used metal substrates. As for the chemical deposition method, which has advantages such as its simple process and equipment, it is merely able to be applied to those metals that are less active than others [10][11][12]. The strong acid and alkali solution is mainly used for the chemical etching for some commercial formations of surface textures. However, the etching stability of the reaction process is poor because of the variation of the concentration, the surface microscopic size, and morphology are difficult to control [13][14].

2. Advantages of Fluoro-Modified Polyurethane

Polyurethane has the advantages of wear resistance, tear resistance, flex resistance, etc. over many other coating materials, but it also has disadvantages, because the bubbles are easily trapped in the polyurethane due to its long curing process and high surface energy. The copolymerization of silicone and polyurethane can address these defects; e.g., using polydimethylsiloxane (PDMS) reacted with isocyanates or prepolymer formed a silicone–polyurethane copolymer through addition polymerization and a chain-extension reaction [15]. Besides, the advanced siloxane-modified polyurethane with polyamino functional groups in the side chain was also used to further enhance its original performance [16]. The amino siloxane attached as the side chain of the polyurethane could be conducive to the migration of silicon atoms to the surface and effectively improve the surface and mechanical properties of the polyurethane [17][18][19]. Although the surface energy of polysiloxane is already very small, perfluoroalkane could be even half of the polysiloxane. Therefore, the introduction of perfluoroalkyl groups into the chain of polysiloxane could not only make the surface energy as low as fluorine, but the flexibility and softness could also become similar to that of silicone [20][21][22].

In previous attempts of fabricating piping materials and preparing marine coatings, it is found that the modification of the surface material and deposition of a coating with low surface energy at the original surface material can also significantly reduce the flow resistance. The lateral adhesion force between a liquid drop and a solid can also be divided into static and kinetic regimes. With the decrement of the surface energy and increment of the superhydrophobicity, the lateral adhesion force between the liquid and the surface would be reduced, and the drops would start sliding over solid surface easily [23]. Besides, the spatial surface structures formed by chemical etching and the substitution reaction would also enhance the drag-reduction effect. As the roughness increased, the threshold force to initiate the drop motion would decrease [24]. Hence, the combination of a chemical etching method and a proper coating material could not only extend the original mechanical and chemical durability by the protective coating, but its surface structure advantages could also be reserved [25]. Moreover, the drag-reduction performance of the substrate could be further enhanced. The durability of the surface, especially the chemical

durability probed by immersion in liquids, is also another factor to consider regarding the fabrication. Polyvinylidene fluoride (PVDF), polytetrafluoroethylene (PTFE), and polydimethylsiloxane (PDMS) are the typical materials that are being used in the fabrication of low surface energy coating, while the superhydrophobic fluoro-polyurethane surface and its drag-reduction behavior have been seldom documented [26][27][28][29].

3. Chemical-Etching Enhancement of Fluoropolyurethane

The 30 mm × 30 mm zinc substrate was rinsed with acetone 5 times and ultrasonically cleaned in deionized water for 15 min. After being dried in the oven at 100 °C for 30 min, the samples were etched by a mixing solution with 5.0 mL of nitric acid, 30.0 mL of distilled water, and 1.0 g of copper nitrate for 60 s at 60.0 °C. Finally, these samples were rinsed thoroughly with deionized water and dried at 100 °C for another 30 min.

Methyl Fluoro-Aminopropyl Polydimethyl Siloxane (MF-APS) was synthesized by Methyl perfluorooctadecanoate (PC5139M) and aminopropyl polydimethylsiloxane (APS) droplets under 50 °C and stirred at 6.7 s^{-1} for 2.5 h. After the vacuum distillation of the previous substituted process, the PPG were treated together with MF-APS by vacuum dehydration at 25 °C for another 10 min (**Figure 1**). Then, a proper amount of xylene and excess 2,4-toluene diisocyanate (TDI) were added into the dehydrated mixture, preheated, and reacted for another 2.5 h at 90 °C to synthesize the isocyanate-terminated polyurethane prepolymer [30]. After the synthesis of polyurethane prepolymer, the melted 3,3'-dichloro-4, 4'-Diamino-diphenylmethane (MOCA) was added in and stirred at 13.3 s^{-1} for 60 s. Finally, the reacted fluropolyurethane was sprayed on the etched/unetched zinc substrate, cured at 60 °C for 7 days, and then dried at room temperature for another day to prepare fluoropolyurethane treated drag-reduction surface material. Furthermore, the etched zinc substrate capped with fluoropolyurethane and unetched zinc substrate capped with and w/o fluoropolyurethane were the test surfaces, while the unetched zinc substrate served as the control group in this experiment.

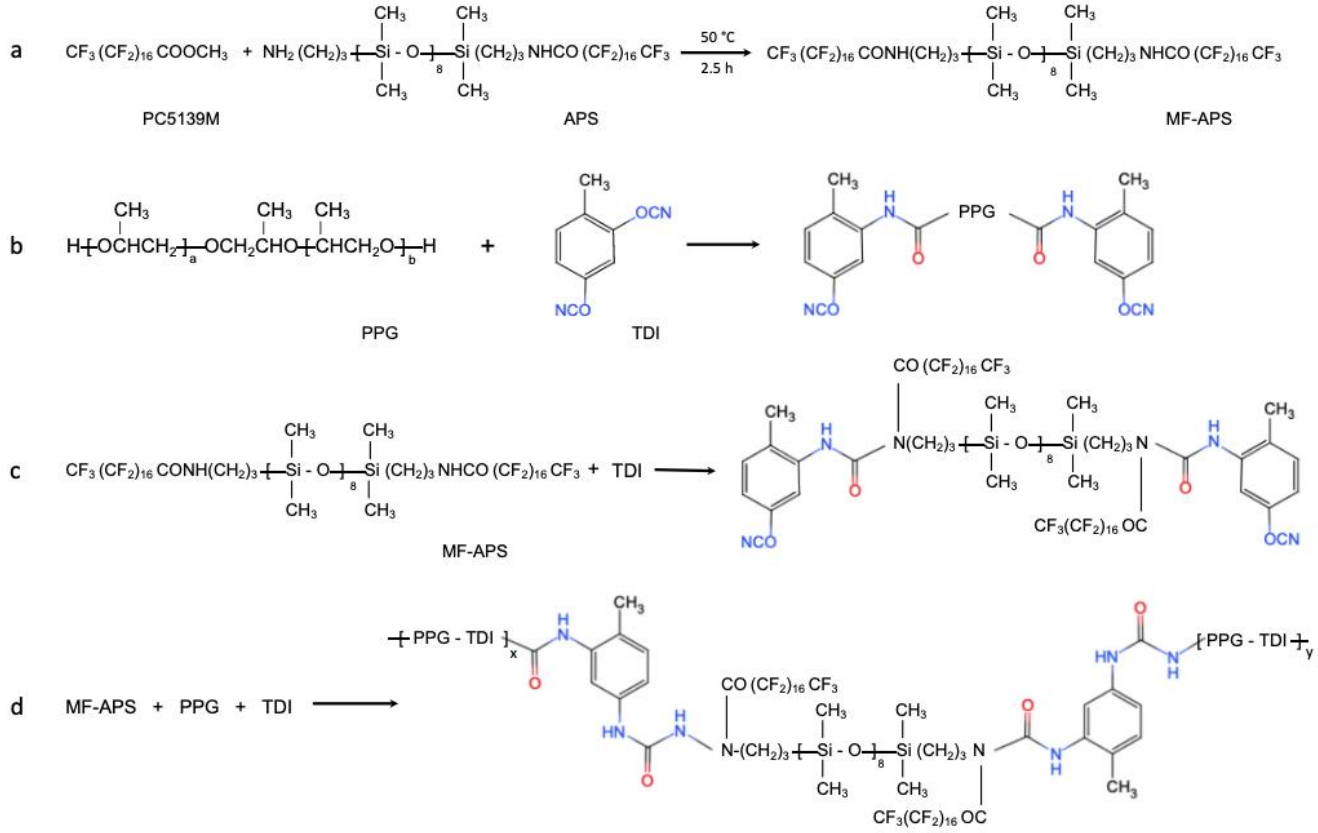

Figure 1. Synthesis of the prepolymer and fluoropolyurethane (a) synthesis of Methyl Fluoro-Aminopropyl Polydimethyl Siloxane (MF-APS), (b) prepolymer produced by polypropylene glycol (PPG) and 2,4-toluene diisocyanate (TDI), (c) prepolymer produced by MF-APS and TDI, and (d) synthesis of prepolymer end-capped by an -NCO group.

4. Microchannel Drag-Reduction Analysis of Chemical-Etching Enhanced Surface

The uncertainty/error and parameters of the non-standard design microchannel are indicated in **Table 1**. Only the stable and unchanged reading would be recorded for each variation of microchannel height as well as Reynolds number.

Table 1. Uncertainty/error and parameters of non-standard design microchannel

Parameters of Non-standard Design Microchannel	Set Value (SV)
Microchannel parameter and dimensions	100 mm × 20 mm × variable h; jet inlet/outlet: r = 5 mm , h = 10 mm
Volume flow rate	1×10^{-5} to 7×10^{-5} m^3/s
Static pressure	0–2.5MPa
Fluids property	DI water: ρ = 998.2 kg/m^3, viscosity 1.00 mPa·s;
Analogy method	Finite volume method
Solution method	Pressure-cased solver
Algorithm	PISO
Inlet condition	Velocity-inlet
Outlet condition	Free discharge
Test surface	(a) Unetched zinc substrate, (b) Unetched zinc + fluoropolyurethane, (c) Cu^{2+}/ HNO_3 etched zinc, and (d) Cu^{2+}/ HNO_3 etched zinc + fluoropolyurethane

In the experiment, since it is not a circular pipe, the equivalent diameter W' = 2Wh/(W + h) was used, where W = 10 mm and variable h were the width and height of the microchannel. In order to observe the actual flow-resistance effect, the pressure drop must be tested at the same Reynolds number. The Reynolds number (Re) is a dimensionless number that can be used to characterize fluid flow, which is expressed as Re, Re = ρvd/μ, where v, ρ, μ are the flow velocity, density, and viscosity coefficient of the fluid, respectively. As d was supposed to be the feature-length of the microchannel, so the W' was also used as the 'feature-length' (d) in calculating Re. The use of Reynolds numbers to distinguish fluid flow was laminar or turbulent and can also be used to determine the resistance to flow of an object in a fluid.

Firstly, it is measured under the condition of water inlet pressure by taking the readings of the cylinder and pressure meters on the microchannel. Comparing to the relationship of the pressure drop according to the increment of Reynolds number, the diagram as shown in **Figure 2** was finally generated. The trendline indicated the laminar flow regions under the height of 192.53 μm, which should be in between Re = 0 and Re = 580. As the Reynolds number at the horizontal ordinate was constant, the less the pressure dropped, the less flow resistance the surface should have. Therefore, it could be observed that the pressure drops of these fluoropolyurethane-capped zinc substrates were smaller than those of the unetched zinc substrate at the same Reynolds number, which indicted a better drag reduction effect. Moreover, as the Reynolds number increased under the same channel height, the drag reduction effect would increase slightly as well.

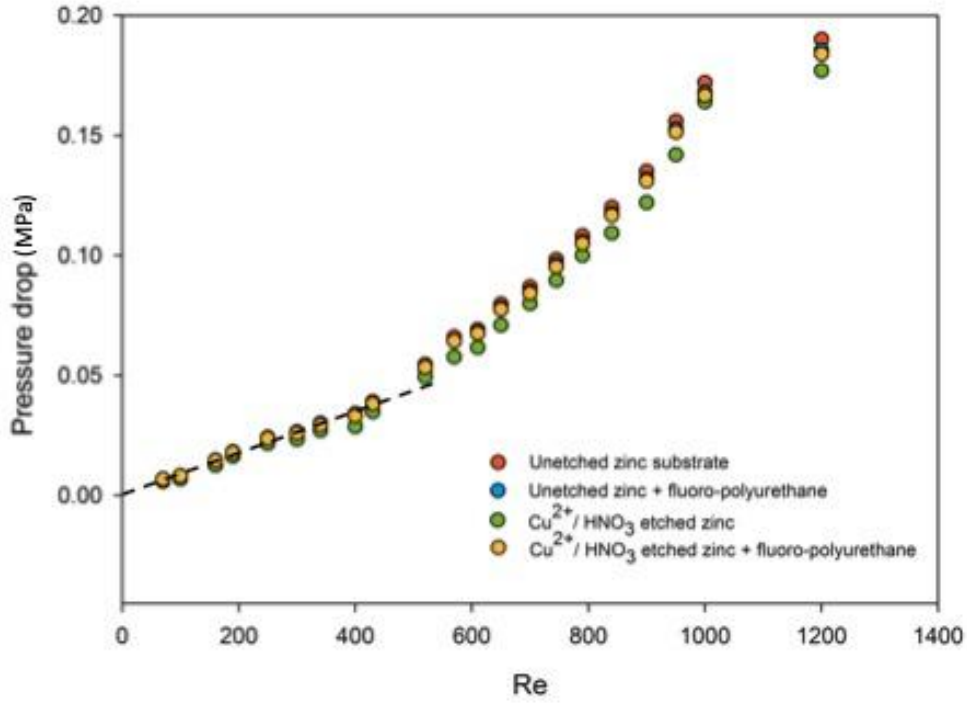

Figure 2. Pressure drop–Reynolds number diagram at h = 192.53 μm microchannel height.

Then, comparing with the unetched zinc substrate (control group), the drag reduction rate of the superhydrophilic and superhydrophobic zinc substrate were made. The drag reduction rate (%) was calculated. Diagrams of the drag reduction rate (%) over Reynolds number, for a total of 21 points, were plotted for each zinc substrate group. It could be observed that the superhydrophilic drag-reduction rate was decreased with the increment of the Reynolds number. The superhydrophobic drag reduction rate in the all flow zone was basically maintained at about 3.16%, as shown in Figure 3.

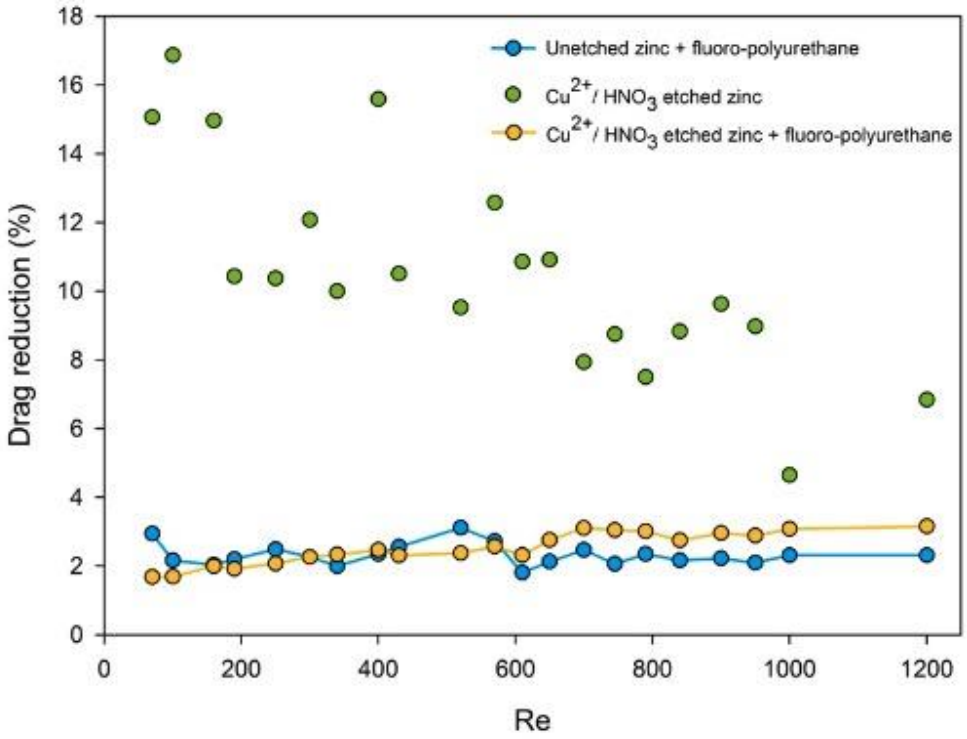

Figure 3. Drag-reduction rate–Reynolds number diagram of the superhydrophilic/hydrophobic surface compared with an unetched zinc substrate at h = 192.53 μm.

After each Reynolds-number group under h = 192.53 μm drag-reduction test was finished, the height of the channel was adjusted to reduce or increase by tightening the screws at h = 122.21 μm and h = 277.48 μm, respectively. Measurements were taken to obtain the pressure drop and Reynolds number data of different zinc substrates. Comparing the Reynolds number and pressure drop diagrams tested under different channel heights, two sets of pressure drop Reynolds number relationship diagrams were generated also, and all the data were under the same pattern [31].

It is known from Figure 4 that the resistances of all the surfaces were changed by varying the microchannel height. Under all the flow regions, from laminar to turbulent, both the superhydrophilic and superhydrophobic surfaces indicated certain drag-reduction effects. With the decrement of the flow rate or the increment of channel height, the superhydrophilic drag reduction rate became smaller, and the superhydrophobic drag reduction rate remained unchanged at around 4.0%, which was relatively stable. As for the superhydrophobic surface fabricated in this paper, it is generally believed that there is a non-shear air/water interface on the low Van der Waals force, and the fluid can shear freely at the gas-liquid interface with almost no resistance, which results in wall slippage, a lower friction coefficient, and flow resistance [32][33][34]. Since the air was also able to be dissolved in the water, the non-shear air-water interface was formed by the separated air and the coating surface during the time that water flew over. Hence, for those etched surfaces, water molecules could not directly contact the surface of the fluoropolyurethane, and these surface characteristics could reduce the friction factor**.** As for continuously increasing the Reynolds number and flow rate, the non-shear air-water interface might become thinner and thinner [35][36].

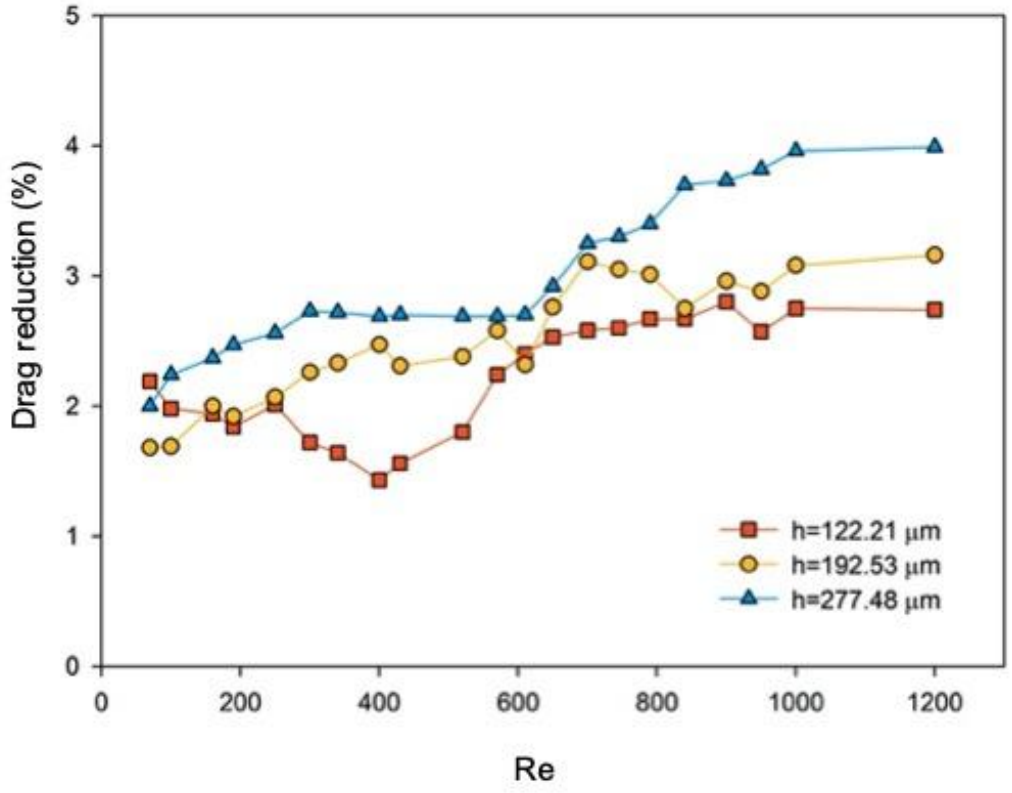

Figure 4. Cu^{2+}/HNO_3- etched zinc + fluoropolyurethane drag reduction rate at different channel heights and Reynolds numbers.

However, the superhydrophilic drag reduction effect was even more obvious than the superhydrophobic. This interesting and repeatable scenario was supposedly caused by the ripple effect regarding the dissolved gas with higher affinity and electrical polarization sticking to the superhydrophilic surface than the superhydrophobic one, an achievement of microbubble drag reduction by the structure change of the boundary layer [35][36][37][38], and surface abrasion that resulted from high fluid velocity and enabled the substituted copper particles rolling near the wall surface. This causality is still under further analysis through experimental and modeling methodology separately in ongoing work [39][40].

To conclude, the main achievement of this research regards the aspects of the novel modification of the polyurethane-coating system, the good combination between an inorganic substrate and organic coating for drag reduction, the new methodology for a flow resistance test in the microchannel, and inclusive discussion about the drag-reduction effect and mechanisms with the latest research findings. As it was known to date, superhydrophobic, hierarchical, nanotextured polymerics were applied to the surface to enhance its superhydrophobicity and drag-reduction effect [41][38]. However, the adhesion force between the organic-coating matrix and the public use metal surface is still low for most polymeric coatings. When the pressure impact on the surface becomes higher, the surface texture would be certainly destroyed, and the coating layer would be even peeled off [42][43][44][45][46]. In this study, the polyurethane-based coating system, which had good adhesion with zinc substrates, was fluoro-modified and then applied in the microchannel for the flow resistance test. The microchannel

was designed with variable height and extremely small ratios between the length, width, and height. The experimental result and mechanism analysis indicated that at low Reynolds number flow conditions, the surface texture friction and intermolecular forces between water and fluoropolyurethane would be the main factors that influenced the drag reduction, while at high Reynolds numbers, the low surface energy and the slight non-shear air-water interface would dominate the drag-reduction effect.

5. Position View of Drag-reduction Enhancement Methodology by Chemical Etching

This paper proposed a fast method to fabricate a superhydrophobic and low flow-resistance fluoropolyurethane surface. Its drag-reduction effect could be further enhanced by the micro-nano scale structures on the zinc substrate, which was formed by the copper-ion assisted nitric acid etching on the zinc substrate via a simple process. As expected, the micro-nano structures obtained by chemical etching could contribute to the enhancement of the superhydrophobicity of the surface characters and low flow resistance. As this newly fabricated surface was applied to a non-standard design microchannel, the drag reduction rate remained basically unchanged at 4.0% with all variations of Reynolds numbers. Furthermore, the prepared superhydrophobic surface exhibited outstanding surface durability when it was immersed in solutions of acid, alkali, and salt.

References

1. Ma, M.; Randal, M.; Superhydrophobic surfaces. *Curr. Opin. Colloid Interface Sci.* **2006**, *11*, 193–202.
2. L. Feng; S. Li; Y. Li; H. Li; L. Zhang; J. Zhai; Y. Song; B. Liu; Lei Jiang; D. Zhu; et al. Super-Hydrophobic Surfaces: From Natural to Artificial. *Advanced Materials* **2002**, *14*, 1857-1860, 10.1002/adma.200290020.
3. W. Barthlott; Christoph Neinhuis; Purity of the sacred lotus, or escape from contamination in biological surfaces. *Planta* **1997**, *202*, 1-8, 10.1007/s004250050096.
4. Cecile Cottin-Bizonne; Jean-Louis Barrat; L. Bocquet; Elisabeth Charlaix; Low-friction flows of liquid at nanopatterned interfaces. *Nature Materials* **2003**, *2*, 237-240, 10.1038/nmat857.
5. S.M.M Ramos; E Charlaix; A Benyagoub; Contact angle hysteresis on nano-structured surfaces. *Surface Science* **2003**, *540*, 355-362, 10.1016/s0039-6028(03)00852-5.
6. Donghyun Kim; Woonbong Hwang; Hyun C Park; Kun-H Lee; Superhydrophobic nano-wire entanglement structures. *Journal of Micromechanics and Microengineering* **2006**, *16*, 2593-2597, 10.1088/0960-1317/16/12/011.
7. Wensheng Fu; Yufang Luo; JingJin Tan; Bohan Jiang; Research Progress of Superhydrophobic Polymer Composite Coatings for os Magnesium Alloys. *Journal of Metallic Material Research*

2020, *3*, 22, 10.30564/jmmr.v3i1.1753.

8. Feng, L.; Song, Y.; Zhai, J.; Liu, B.; Xu, J.; Jiang, L.; Zhu, D.; Creation of a super- hydrophobic surface from an amphiphilic polymer. *Angew. Chem. Int. Ed.* **2003**, *42*, 800-802.
9. Kosmas Ellinas; Angeliki Tserepi; Evangelos Gogolides; Superhydrophobic, passive microvalves with controllable opening threshold: exploiting plasma nanotextured microfluidics for a programmable flow switchboard. *Microfluidics and Nanofluidics* **2014**, *17*, 489-498, 10.1007/s10404-014-1335-9.
10. Tadanaga, K.; Morinaga, J.; Matsuda, A.; Minami, T.; Super-hydrophobic–super- hydrophilic micropatterning on flowerlike alumina coating film by the sol–gel method. *Chem. Mater.* **200**, *12*, 590-592.
11. Jeffrey P. Youngblood; Thomas J. McCarthy; Ultrahydrophobic Polymer Surfaces Prepared by Simultaneous Ablation of Polypropylene and Sputtering of Poly(tetrafluoroethylene) Using Radio Frequency Plasma. *Macromolecules* **1999**, *32*, 6800-6806, 10.1021/ma9903456.
12. Liu, H.; Feng, L.; Zhai, J.; Jiang, L.; Zhu, D.; Reversible wettability of a chemical vapor deposition prepared ZnO film between super-hydrophobicity and super- hydrophilicity. *Langmuir* **2004**, *20*, 5659-5661.
13. Tomoki Hirano; Kazuki Nakade; Shaoxian Li; Kentaro Kawai; Kenta Arima; Chemical etching of a semiconductor surface assisted by single sheets of reduced graphene oxide. *Carbon* **2018**, *127*, 681-687, 10.1016/j.carbon.2017.11.053.
14. Yugui Jiang; Zhiqiang Wang; Xi Yu; Feng Shi; Huaping Xu; Xi Zhang; Mario Smet; Wim Dehaen; Self-Assembled Monolayers of Dendron Thiols for Electrodeposition of Gold Nanostructures: Toward Fabrication of Superhydrophobic/Superhydrophilic Surfaces and pH-Responsive Surfaces. *Langmuir* **2005**, *21*, 1986-1990, 10.1021/la047491b.
15. Chong Cheen Ong; Satisvar Sundera Murthe; Norani Muti Mohamed; Veeradasan Perumal; Mohamed Shuaib Mohamed Saheed; Nanoscaled Surface Modification of Poly(dimethylsiloxane) Using Carbon Nanotubes for Enhanced Oil and Organic Solvent Absorption. *ACS Omega* **2018**, *3*, 15907-15915, 10.1021/acsomega.8b01566.
16. Zhen Ge; Yunjun Luo; Synthesis and characterization of siloxane-modified two-component waterborne polyurethane. *Progress in Organic Coatings* **2013**, *76*, 1522-1526, 10.1016/j.porgcoat.2013.06.007.
17. C. Philipp; Steven Eschig; Waterborne polyurethane wood coatings based on rapeseed fatty acid methyl esters. *Progress in Organic Coatings* **2012**, *74*, 705-711, 10.1016/j.porgcoat.2011.09.028.
18. D.K. Chattopadhyay; K. V. S. N. Raju; Structural engineering of polyurethane coatings for high performance applications. *Progress in Polymer Science* **2007**, *32*, 352-418, 10.1016/j.progpolymsci.2006.05.003.

19. Aiswarea Mathew; Surendra Kurmvanshi; Smita Mohanty; Sanjay K. Nayak; Preparation and characterization of siloxane modified: Epoxy terminated polyurethane-silver nanocomposites. *Polymer Composites* **2017**, *39*, E2390-E2396, 10.1002/pc.24708.
20. Teluka P. Galhenage; Augusto M. S. Moreira; Ryan J. Burgett; Shane J. Stafslien; John A. Finlay; Sofia C. Franco; Anthony S. Clare; Dean C Webster; Lyndsi Vanderwal; Poly(ethylene) glycol-modified, amphiphilic, siloxane–polyurethane coatings and their performance as fouling-release surfaces. *Journal of Coatings Technology and Research* **2016**, *14*, 307-322, 10.1007/s11998-016-9862-9.
21. Yuanzhe Li; Zhe Cui; Qiucheng Zhu; Srikanth Narasimalu; Zhili Dong; Fabrication of Zinc Substrate Encapsulated by Fluoropolyurethane and Its Drag-Reduction Enhancement by Chemical Etching. *Coatings* **2020**, *10*, 377, 10.3390/coatings10040377.
22. Aqdas Noreen; Khalid Mahmood Zia; Shazia Tabasum; Waseem Aftab; Muhammad Shahid; Mohammad Zuber; Structural elucidation and biological aptitude of modified hydroxyethylcellulose-polydimethyl siloxane based polyurethanes. *International Journal of Biological Macromolecules* **2020**, *150*, 426-440, 10.1016/j.ijbiomac.2020.01.288.
23. Nan Gao; Florian Geyer; Dominik W. Pilat; Sanghyuk Wooh; Doris Vollmer; Hans-Jürgen Butt; Rüdiger Berger; How drops start sliding over solid surfaces. *Nature Physics* **2017**, *14*, 191-196, 10.1038/nphys4305.
24. Panagiotis Sarkiris; Kosmas Ellinas; Dimitris Gkiolas; Dimitrios Mathioulakis; Evangelos Gogolides; Motion of Drops with Different Viscosities on Micro-Nanotextured Surfaces of Varying Topography and Wetting Properties. *Advanced Functional Materials* **2019**, *29*, 1902905, 10.1002/adfm.201902905.
25. Guillaume Lagubeau; Marie Le Merrer; Christophe Clanet; David Quéré; Leidenfrost on a ratchet. *Nature Physics* **2011**, *7*, 395-398, 10.1038/nphys1925.
26. Kosmas Ellinas; A. Tserepi; Evangelos Gogolides; Durable superhydrophobic and superamphiphobic polymeric surfaces and their applications: A review. *Advances in Colloid and Interface Science* **2017**, *250*, 132-157, 10.1016/j.cis.2017.09.003.
27. 伟 罗; Progress of Research on the Boundary Slip of Fluid Flows at the Micro-Nanometer Scale. *Advances in Porous Flow* **2013**, *3*, 9-13, 10.12677/apf.2013.31002.
28. Hamed Esmaeilzadeh; Keqin Zheng; Junwei Su; Joey Mead; Margaret J. Sobkowicz; Hongwei Sun; Experimental Study of Drag Reduction on Superhydrophobic Surfaces Using Quartz Crystal Microbalance (QCM). *Volume 6: Energy* **2017**, *null*, , 10.1115/imece2017-72314.
29. Poetes, R.; Holtzmann, K.; Franze, K.U. Steiner, Metastable underwater superhydrophobicity. Phys. Rev. Lett. 2010, 105, 166104.

30. Yuanzhe Li; Boyang Luo; Claude Guet; Srikanth Narasimalu; Zhili Dong; Preparation and Formula Analysis of Anti-Biofouling Titania–Polyurea Spray Coating with Nano/Micro-Structure. *Coatings* **2019**, *9*, 560, 10.3390/coatings9090560.
31. N. K. Madavan; S. Deutsch; C. L. Merkle; Measurements of local skin friction in a microbubble-modified turbulent boundary layer. *Journal of Fluid Mechanics* **1985**, *156*, 237, 10.1017/s0022112085002075.
32. Arjun, K.; Rakesh, K. CFD analysis of thermal performance of microchannel nanofluid flow at different Reynolds numbers. Songklanakarin J. Sci. Technol. 2019, 41, 109–116.
33. Elizaveta Ya Gatapova; Dmitry S. Gluzdov; A.O. Zholanova; The Drag Reduction Of Microchannel Flow by Contrast Wettability. *MATEC Web of Conferences* **2016**, *72*, 1030, 10.1051/matecconf/20167201030.
34. Jihui Huang; Yujun Deng; Peiyun Yi; Linfa Peng; Experimental and numerical investigation on thin sheet metal roll forming process of micro channels with high aspect ratio. *The International Journal of Advanced Manufacturing Technology* **2018**, *100*, 117-129, 10.1007/s00170-018-2606-5.
35. Doyoung Byun; Jihoon Kim; Han Seo Ko; Hoon Cheol Park; Direct measurement of slip flows in superhydrophobic microchannels with transverse grooves. *Physics of Fluids* **2008**, *20*, 113601, 10.1063/1.3026609.
36. S. Deutsch; J. Castano; Microbubble skin friction reduction on an axisymmetric body. *Physics of Fluids* **1986**, *29*, 3590, 10.1063/1.865786.
37. Y. L. Zhou; H. Chang; Numerical simulation of hydrodynamic and heat transfer characteristics of slug flow in serpentine microchannel with various curvature ratio. *Wärme- und Stoffübertragung* **2019**, *55*, 3343-3358, 10.1007/s00231-019-02664-4.
38. Dimitrios P. Papageorgiou; Katerina Tsougeni; Angeliki Tserepi; Evangelos Gogolides; Superhydrophobic, hierarchical, plasma-nanotextured polymeric microchannels sustaining high-pressure flows. *Microfluidics and Nanofluidics* **2012**, *14*, 247-255, 10.1007/s10404-012-1043-2.
39. Huo, S.; Yu, Z.; Li, Y. Flow characteristics of water in superhydrophobic microchannels. Chem. J. China 2007, 58, 2721–2726.
40. Peichun Tsai; Alisia M. Peters; Christophe Pirat; Matthias Wessling; Rob G. H. Lammertink; Detlef Lohse; Quantifying effective slip length over micropatterned hydrophobic surfaces. *null* **2009**, *null*, , null.
41. Kosmas Ellinas; Angeliki Tserepi; Evangelos Gogolides; Superhydrophobic, passive microvalves with controllable opening threshold: exploiting plasma nanotextured microfluidics for a programmable flow switchboard. *Microfluidics and Nanofluidics* **2014**, *17*, 489-498, 10.1007/s10404-014-1335-9.

42. Shuaijun Pan; Arun K. Kota; Joseph M. Mabry; Anish Tuteja; Superomniphobic Surfaces for Effective Chemical Shielding. *Journal of the American Chemical Society* **2012**, *135*, 578-581, 10.1021/ja310517s.
43. Ellinas, K.; Pujari, S.; Dragatogiannis, D.; Charitidis, C.; Tserepi, A. Zuilhof, Plasma micro-nanotextured, scratch, water and hexadecane resistant, superhydrophobic, and superamphiphobic polymeric surfaces with perfluorinated monolayers. ACS Appl. Mater. Interfaces 2014, 6, 6510–6524.
44. Xia Zhang; Yonggang Guo; Hengzhen Chen; Wenzhong Zhu; Pingyu Zhang; A novel damage-tolerant superhydrophobic and superoleophilic material. *Journal of Materials Chemistry A* **2014**, *2*, 9002-9006, 10.1039/c4ta00869c.
45. Huaiyuan Wang; Zhanjian Liu; Enqun Wang; Xiguang Zhang; Ruixia Yuan; Shiqi Wu; Yanji Zhu; Facile preparation of superamphiphobic epoxy resin/modified poly(vinylidene fluoride)/fluorinated ethylene propylene composite coating with corrosion/wear-resistance. *Applied Surface Science* **2015**, *357*, 229-235, 10.1016/j.apsusc.2015.09.017.
46. Xiaotao Zhu; Zhaozhu Zhang; Xuehu Men; Jin Yang; Kun Wang; Xianghui Xu; Xiaoyan Zhou; Qunji Xue; Robust superhydrophobic surfaces with mechanical durability and easy repairability. *Journal of Materials Chemistry* **2011**, *21*, 15793, 10.1039/c1jm12513c.
47. Xiaotao Zhu; Zhaozhu Zhang; Xuehu Men; Jin Yang; Kun Wang; Xianghui Xu; Xiaoyan Zhou; Qunji Xue; Robust superhydrophobic surfaces with mechanical durability and easy repairability. *Journal of Materials Chemistry* **2011**, *21*, 15793, 10.1039/c1jm12513c.